Published in final edited form as:
J Manipulative Physiol Ther. 2011 September ; 34(7): 420–431. doi:10.1016/j.jmpt.2011.05.005.

Relationships between joint motion and facet joint capsule strain during cat and human lumbar spinal motions

Allyson Ianuzzi, PhD,
Department of Biomedical Engineering, Stony Brook University

Joel G Pickar, DC, PhD, and
Palmer Center for Chiropractic Research, Palmer College of Chiropractic

Partap S Khalsa, DC, PhD, DABCO
Department of Biomedical Engineering, Stony Brook University, Program Officer, Division of Extramural Research, National Center for Complementary and Alternative Medicine (NCCAM), National Institutes of Health (NIH)

Abstract

Objective—The lumbar facet joint capsule (FJC) is innervated with mechanically sensitive neurons and is thought to contribute to proprioception and pain. Biomechanical investigations of the FJC have commonly used human cadaveric spines, while combined biomechanical and neurophysiological studies have typically used non-human animal models. The purpose of this study was develop mathematical relationships describing vertebral kinematics and facet joint capsule strain in cat and human lumbar spine specimens during physiological spinal motions in order to facilitate future efforts at understanding the mechanosensory role of the FJC.

Methods—Cat lumbar spine specimens were tested during extension, flexion and lateral bending. Joint kinematics and FJC principal strain were measured optically. FJC strain-intervertebral angle (IVA) regression relationships were established for the three most caudal lumbar joints using cat (current study) and human (prior study) data. FJC strain-IVA relationships were utilized to estimate cat and human spine kinematics that corresponded to published sensory neuron response thresholds for low threshold mechanoreceptors (5% and 10%).

Results—Significant linear relationships between IVA and strain were observed for both human and cat during motions that produced tension in the FJCs ($p<0.01$). During motions that produced tension in the FJCs, the models predicted that FJC strain magnitudes corresponding to published sensory neuron response thresholds would be produced by IVA magnitudes within the physiological range of lumbar motion.

Conclusions—Data from the current study support the proprioceptive role of lumbar spine FJC and low threshold mechanoreceptive afferents, and can be utilized in interpreting combined neurophysiological and biomechanical studies of cat lumbar spines.

CORRESPONDING AUTHOR CONTACT INFORMATION: Allyson Ianuzzi, PhD, Allyson_ianuzzi@yahoo.com, 1302 Wrights Lane East, West Chester, PA 19380, 610-719-5298.

CONFLICTS OF INTEREST
No conflicts of interest were reported for this study.

Introduction

Lumbar facet joints serve mechanical and mechanosensory functions in the spine. The capsule of the facet joint (FJC) contributes to the joint's stability by helping to constrain its motion.[1–2] The FJC is also innervated with low and high threshold mechanically-sensitive neurons.[3–5] These mechanical and sensory characteristics suggest that the FJC may be functionally involved in pain and proprioception.[3, 6] As such, the lumbar FJC is a target for impulse loads delivered during high velocity, low amplitude spinal manipulation (HVLA-SM).[7]

The cat is a commonly used animal model for neuromechanical studies. Substantial neurophysiological background data exist for this species. Its lumbar spine is sufficiently large to obtain biomechanical measurements from paraspinal tissues while simultaneously measuring neural activity in either the lumbar dorsal roots or spinal cord arising from paraspinal mechanoreceptors.[8–9] Neurophysiological studies conducted in the cat,[9–10] as well as biomechanical studies in the human spine,[11] have explored the neuromechanical basis for the observed clinical benefits of HVLA-SM. Lumbar intervertebral motion and FJC strain have been measured in both human and cat lumbar spines during HVLA-SM.[11–12] A relationship between the two species has been described, which can be used to help extrapolate to humans results obtained from neuromechanical studies performed in cats. While such a framework has been developed to evaluate the FJC's role during application of an HVLA-SM,[12] similar comparisons between cat and human spines have not been made for evaluating functions of the lumbar facet joint capsule (e.g., proprioception) during physiological spinal motion.

The purpose of the current study was to develop mathematical relationships describing vertebral kinematics and facet joint capsule strain in cat and human lumbar spine specimens during physiological spinal motions in order to facilitate future efforts at understanding the mechanosensory role of the FJC. The current study describes kinematic testing of cat spine specimens and compares these data to those obtained from human spine specimens in a prior study.[1] We hypothesized that there would be a linear relationship between FJC strain and intervertebral motion in cat and human spine specimens. A regression relationship was developed and validated using statistical tests, and its applicability was demonstrated using previously published response thresholds for mechanoreceptors.[13–14]

Methods

Specimen preparation

Laboratory bred, skeletally mature cats (male, n = 6; mass = 4.1 ± 0.1 kg) were obtained and the lumbar spines (L2 - sacrum; cats have 7 lumbar vertebrae) procured using methods that were in accordance with the Stony Brook University Institutional Animal Care and Use Committee and the Panel on Euthanasia of the American Veterinary Medical Association. L2-sacrum specimens were chosen because the human spine data with which the regression relationships would be developed had been obtained in prior studies using multi-segment specimens (T12-sacrum).[1] This approach of using multi-segmented spine specimens has also been used in studies investigating FJC strain in caudal joints.[12, 15–17] Specimens were dissected under low magnification (10x) to remove all superficial skin, fascia, and muscle, resulting in "osteoligamentous" spine specimens. Care was taken to remove all tissue from the FJC surface such that the capsular ligament was not damaged. Specimens were potted at the sacrum using a polyester resin (Bondo™) such that the vertebral endplates were horizontal with the testing surface.

To enable FJC strain and vertebral kinematic measurements, the specimens were prepared as follows. Black markers were affixed to the surfaces of the L5–6, L6–7 and L7-S1 facet joint capsules. In addition, a small amount of silicon carbide particles was dusted on the surface of each FJC to create a stochastic pattern when illuminated with a fiber optic light. Three infrared reflective markers were attached in a non-collinear fashion to each transverse process at L5, L6 and L7.

Experimental setup

The experimental setup consisted of a mechanical testing apparatus, a camera system consisting of two CMOS cameras to measure FJC strain in three dimensions (MotionPro 500, Redlake, San Diego, CA), and a commercial kinematic system for tracking vertebral kinematics (Qualysis MotionPro cameras and Track Manager System; Innovision Systems, Inc., MI; see Fig. 1). The two camera systems were calibrated before placing the cat spine specimen in the testing apparatus.

Cat lumbar spine specimens (L1 – S1) were attached to a testing plate at the potted sacrum (Fig. 1 top). The most cephalic vertebra (L2) was coupled to a linear actuator (Model 317, Galil, Inc., CA) placed in-series with a force transducer (Model LCF300; Futek, CA, Range ±110 N) to general flexion, extension or lateral bending. A U-shaped coupling was attached to the actuator and to the specimen so that when the actuator displaced the spine, a moment was not induced at the point of application (Fig. 1). The height of the actuator was adjusted such that the actuator was horizontal at peak displacement. Low-friction structural supports (not shown) were added to guide the actuator and minimize off-axis loading of the L2 vertebra during actuation. Applied moment was calculated from applied force and position of each intervertebral joint by static equilibrium as subsequently described under Data Analysis. No buckling of the spine or soft tissues was observed. As performed previously in prior studies from our laboratory,[1, 15, 18] as well as by others,[19] an offset load was applied to the cephalic-most vertebra of a lumbar spine specimen using displacement control, which has been shown to generate facet motion similar to that estimated *in vivo* in a quadruped animal.[19]

Mechanical testing protocol

Mechanical testing consisted of 10 triangular displacement cycles at 10 mm/s to peaks of 10, 20, 30, 40, and 50 mm. These displacement magnitudes were selected because they resulted in maximum moments below the cat spine's torque-limits (approximately 1–2 Nm at L7-S1).[15] The commercial kinematic system was utilized to track the displacements of the markers attached to the L5, L6 and L7 transverse processes. To enable FJC strain measurements for a given specimen and trial, the CMOS cameras were focused on a single FJC (e.g., L5–6) on the right side of the spine. Mechanical testing for the five displacement magnitudes during flexion, extension, and left and right lateral bending ensued. Then, cameras were repositioned and focused on the next FJC (L6–7), the camera systems re-calibrated, and mechanical testing repeated. This was repeated for the third FJC (L7-S1). FJC images were acquired at 25 Hz.

Data analysis

Intervertebral angle (IVA) was calculated from the three-dimensional displacements of the markers on the transverse processes. For each trial, IVA was computed using the method of Soderkvist and Wedin,[20] where IVA at L5–6 and L6–7 was calculated for the cephalic vertebra relative to the respective caudal vertebra comprising that joint. At L7-S1, it was assumed that the sacrum was fixed. To enable comparisons of IVA in the cat spine with previous measurements in the human spine,[1] rotations in the direction of primary loading (hereafter referred to as major-axis rotations) are reported.

Plane strain of the FJC was computed using the images from the two CMOS cameras, which enabled accounting for out-of-plane motions of the FJC during spine actuation. Images were analyzed using a custom program (Matlab). Briefly, the black markers affixed to the outer boundary of the FJC surface defined a plane comprising the FJC surface. Strain within the plane defined by the markers was measured using the silicone carbide particles as follows. For the first image (image *i*) of the FJC taken by each CMOS camera, this two-dimensional plane was divided into a 3×3 array of subregions. Using computer-aided speckle interferometry,[21] the two-dimensional displacements of these subregions were determined for the subsequent image (image *i+1*) in each camera's view. Principles of photogrammetry[22] were applied to calculate the three-dimensional displacements of each subregion of the FJC. This process was repeated for each of the subsequent images comprising a given trial (*i+1* and *i+2*, etc). The 3D subregion displacements were subsequently used to compute plane strain (ε_{xx}, ε_{yy}, ε_{xy}) and principal strain (E_1 and E_2) as previously described.[1] Thusly, FJC strain was measured while minimizing the number of markers required to define the region of interest. As has been done in prior studies of cervical [23] and lumbar [1, 11, 24] FJC strain, principal strains for each subregion were organized and reported as maximum (tensile) and minimum (compressive) principal strain ($\hat{E}_1$ and $\hat{E}_2$, respectively). Subregion $\hat{E}_1$ and $\hat{E}_2$ at peak displacement were averaged to get a representative value for the FJC.

Peak strain ($\hat{E}_1$ and $\hat{E}_2$), IVA, and load (force or moment) for a given trial were computed as the mean peak value for the last five cycles comprising that trial, where load had reached equilibrium. L5–6, L6–7, and L7-S1 joint moments were computed as the product of the applied peak load and the moment arm (i.e., distance between the point of force application and the center of the FJC for that joint).

Statistics

Multiple analysis of covariance (MANCOVA) was performed using a generalized linear model [25] to determine whether each parameter (developed joint moment, IVA about a given axis, $\hat{E}_1$ and $\hat{E}_2$) was significantly associated with: global displacement magnitude (i.e., peak displacement of the actuator), type of motion (extension/flexion or lateral bending), or joint level (L5–6, L6–7, or L7-S1). IVA-global displacement relationships were evaluated using stepwise polynomial regression.

Regression relationships describing FJC strain for both species were developed using data from the current (cat) and prior (human) [1] studies. Separate regression analyses were conducted for each motion (extension, flexion, left lateral bending and right lateral bending) and joint level (caudal, middle, cephalic). The response variables ($\hat{E}_1$ and $\hat{E}_2$) were evaluated to determine whether they were significantly correlated with IVA. Comparison of linear regression lines was conducted to assess whether the slope coefficient for the cat regression was significantly different from that of the human spines. Because FJC strain was referenced from the neutral posture and was considered zero at this position, the regression relationships did not include an intercept term. The regression relationships developed in the current study were used to estimate the cat IVA magnitudes that corresponded to 5% and 10% strain (i.e., potential low-threshold, Group II mechanoreceptor response thresholds). SigmaStat (Version 3.01, Systat, Inc.) and JMP (Version 6.0.0) and were used for statistical tests. Significance levels for MANCOVA and stepwise regression were $\alpha = 0.05$ and 0.10, respectively.

Results

Joint moment

There were significant associations between the joint moments that developed and the experimental factors examined: global displacement, joint level, and type of motion, as well as for their interactions (MANCOVA; $p < 0.001$). Joint moment – global spine displacement relationships were nonlinear (Fig. 2). At all three joints, the relationship was best fit with third-order polynomials, except for L6–7 (middle) during extension/flexion which was second order. Relationships were statistically significant (incremental polynomial regression; $p < 0.022$) and highly correlated ($R^2 > 0.73$). Moments developed during lateral bending were significantly greater than those developed during extension-flexion at L5–6 (cephalic) and L6–7 ($p<0.05$).

Intervertebral angle

There were significant associations between IVA and global displacement, as well as for interactions between global displacement-joint level, global displacement-motion type, and global displacement-joint level-motion type (Fig. 3). IVA-global displacement relationships were typically 1st order (linear; incremental polynomial regression; $p < 0.001$) except at L5–6 during extension-flexion and lateral bending (2nd order, $p<0.05$) and L6–7 during extension-flexion (2nd order; $p < 0.05$). Relationships between major-axis IVA and global displacement were well correlated (R^2 range: 0.74–0.97).

Significant ($p<0.001$) third-order moment-IVA relationships were also observed, which had moderate to good correlation (R^2 range: 0.58–0.93; Fig. 4). The joint moments that developed during lateral bending were greater for a given IVA compared to extension-flexion. The range of motion (indicated by the range of IVA magnitudes for each segmental level) during extension-flexion was greater compared to lateral bending.

FJC strain

$\hat{E}_2$-IVA and $\hat{E}_1$-IVA linear regression relationships for the cat (current study) and the human (previous study [1]) are shown in Figs. 5 and 6, respectively. For the cat FJC, there were significant associations between $\hat{E}_2$ (compressive) strain and the experimental factors examined: joint level, motion type, and global displacement magnitude; significant interactions were also observed (Fig. 5; MANCOVA; $p < 0.01$). At L7-S1, $\hat{E}_2$ was significantly greater during extension-flexion compared to lateral bending (Tukey test, $p<0.05$). A similar trend was observed at the other joints, although the difference was not significant.

Slope coefficients for the $\hat{E}_2$ linear regression models are presented for cat (A_C) and human (A_H) spines, as well as the ratio for A_C/A_H, (see Table 1). The relationship between $\hat{E}_2$ and IVA was significant ($p < 0.05$) for both cat and human lumbar spines, with a few exceptions, which overall supported the study hypothesis. Regression relationships tended to be insignificant in the few specimens where the minimum principal strain was positive in sign (i.e., tensile), for example at the caudal joint during flexion or left lateral bending (see Fig. 5, panels in bottom row). Correlation coefficients varied with species, joint level and motion type, and tended to improve at the more caudal joints compared to the cephalic joint for a given motion type and species (Table 1). The slopes of the regression relationship for cat versus human spines were not significantly different except at the middle joint during lateral bending and caudal joint during flexion-extension. At the middle joint, cat FJC $\hat{E}_2$ absolute magnitudes increased more substantially with increasing IVA compared to human FJC $\hat{E}_2$ magnitudes during lateral bending ($p < 0.05$). At the caudal joint, human FJC $\hat{E}_2$ magnitudes

increased more substantially with increasing IVA compared to cat FJC $\hat{E}_2$ magnitudes ($p < 0.05$) during extension-flexion.

There were significant associations between cat FJC $\hat{E}_1$ (tensile) strain and the experimental factors examined (Fig. 6): joint level and displacement magnitude; significant interactions were also observed (MANCOVA; $p < 0.001$). The effect of motion type on cat FJC $\hat{E}_1$ approached significance ($p = 0.06$). Cat FJC $\hat{E}_1$ was significantly greater at L6–7 compared to L5–6 (Tukey test, $p<0.05$).

The slope coefficients for $\hat{E}_1$ versus IVA linear regression models of cat (A_C) and human (A_H) spines, as well as the ratio for A_C/A_H, are presented in Table 2. Again, the majority of regression relationships indicated a significant correlation between $\hat{E}_1$ and IVA ($p < 0.05$), supporting the study hypothesis. There were also several joint levels and motion types where the A_C versus A_H was significantly different. For example at the caudal joint, human FJC $\hat{E}_1$ increased more substantially with increasing IVA compared to cat FJC $\hat{E}_1$ ($p < 0.05$). For other combinations of joint level and motion type, cat FJC $\hat{E}_1$ increased more substantially with increasing IVA compared to human FJC $\hat{E}_1$, although this was not always significant. The correlation coefficients varied with joint level, type of motion and species, and tended to be higher in magnitude at the more caudal joints and during motions that produced tension in the FJC (i.e., flexion and left lateral bending).

The regression relationships were utilized to estimate the magnitude of joint motion (i.e. IVA) that would be required to achieve 5% and 10% strain (i.e., strain magnitudes above anticipated low-threshold, Group II mechanoreceptor response thresholds;[13–14] see Table 3). In both cat and human lumbar spines, at least 5% strain could be achieved within the range of motion for joint motions that produced tension in the FJC (i.e., flexion and lateral bending in a direction contralateral to the side of the FJC).

Discussion

This is the first study to describe *in situ* cat lumbar spine biomechanics and FJC strains and compare them with human spines during physiological spinal motions. Cat spine vertebral kinematics and facet joint capsule (FJC) strain magnitudes were measured during extension-flexion and lateral bending. Joint moment and intervertebral angle (IVA) were correlated with global spine displacement. Joint moment-IVA relationships were nonlinear, similar to human cadaveric spines measured in a prior study.[1] FJC strain-IVA relationships were established for cat lumbar spine specimens and were also established for human cadaveric spines using measurements obtained from the previous study.[1] These relationships were used to associate FJC strain magnitudes in the cat with those in human spine specimens. Significant linear relationships between FJC strain and IVA were established using linear regression in both species. To identify spinal motions that result in similar FJC strain magnitudes in the two species ($\hat{E}_{1,c} = \hat{E}_{1,h}$), the relationship between their respective IVAs can be expressed as $IVA_c/IVA_h = A_h/A_c$, where A is the slope coefficient and subscripts denote human and cat. The regression relationships determined in the current study can be used to extrapolate neurophysiological data from an animal model using the cat lumbar spine to the human in order to estimate how human FJC neurons might respond to biomechanically similar motions.

The *in-situ* cat lumbar spinal motions described here were larger in magnitude than those previously reported by the only analogous *in vivo* cat study to date.[26] From extension to flexion, sagittal range of motion in the L6-sacral region was smaller (~2° at L6–7; ~7.5° at L7-S1) compared to the current study (~14° at L6–7; ~28° at L7-S1), though similar at L5–6 (~7° versus ~6°, respectively). From neutral posture to maximum lateral flexion, IVA

magnitudes at L5–6 through L7-S1 were also smaller in magnitude but only slightly (< 5°) compared to those measured in the current study (~6° at L5–6 and L6–7; ~8° at L7-S1). Differences between these studies could have occurred because only the lumbar spine (from L2 to sacrum) was loaded in the current study, while the entire, intact vertebral column was used in Macpherson and Ye's *in vivo* study. [26] In the current study during extension-flexion, coupled motions of the motion segments of interest were not restricted and did indeed occur. In contrast, Macpherson and Ye manually flexed the spine and made efforts to keep the spine within the focal plane the X-ray device used to measure IVA which likely reduced out-of-plane coupled motions. As a result, a smaller portion of the cat spine's total range of motion during flexion might have been tested in the prior study. This conclusion is supported by the fact that in the current study during lateral bending, the low-friction structural supports used to minimize off-axis loading of L2 during actuation became noticeably engaged. With this apparent reduction in coupled motions, IVA magnitudes we measured during lateral bending were similar to those measured by Macpherson and Ye *in vivo.* [26]

Although the data demonstrated variability, our hypothesis that FJC strain would be linearly related to joint motion was largely supported. Relating FJC strain magnitudes to IVA during extension-flexion and lateral bending often resulted in significant linear regression relationships for both cat and human spines, though the correlations were only weak to moderate. This may be due to our cadaveric human data having been obtained from a prior study where the range of motion tested was small compared to the total range of motion for the human spine.[1] In the current study, associations between cat FJC strain and IVA were improved when larger IVA and FJC strain magnitudes developed. It is possible that within the neutral zone the FJC strain-IVA relationship demonstrates a degree of non-linearity, and that better associations could have been obtained for the human spine's active zone had a larger portion of its range of motion been tested. A 10 Nm torque limit was used in the prior study from which the human strain data were taken.[1] This conservative limit was based on estimates under torque control [15 Nm from [27]]. However, it was recently reported [15] that 15 Nm may be too conservative when testing is performed under displacement control. Torque limit in human lumbar spines during displacement-control is closer to 17.5 Nm.[15] Had a higher torque-limit been chosen in the prior human study where the strain data for the current study were obtained, motions may have resulted in larger FJC strain and IVA magnitudes and improved correlation.

Our selection and use of a testing methodology, where an offset load was applied to the superior-most vertebra of a complete lumbar spine specimen tested under displacement control without an axial compressive load, was supported by comparing data between the current study and prior studies. In a study evaluating dog lumbar spine specimens, an offset load was applied to the most superior vertebra under displacement and moment control, both with and without a compressive axial load.[19] Using this experimental model, facet motion under both displacement and load control were comparable to the *in vivo* condition, and application of an axial load did not significantly affect facet motion.[19] Human FJC strain-IVA relationships from the current study were also compared to those obtained by Panjabi et al. in a single human L4–5 functional spinal unit tested under moment control.[2] From Figure 5 of Panjabi et al.,[2] we calculated the slope of the FJC strain-IVA relationship to be 0.014 %/degree on the right side and 0.0085%/degree on the left side (average: 0.011%/degree), which compares favorably to that reported for L4–5 in the current study (0.017%/degree). Combined, these comparisons with prior studies support our use of a displacement-controlled model.

Prior non-human animal models have been used to evaluate the role of the FJC in spine proprioception utilizing different indicators of joint motion. In a recent study using a goat *in*

vivo model, cervical FJC maximum principal strain magnitudes were measured in response to the application of a controlled vertebral displacement.[28] Applying linear regression analysis to the data points from the nine defined regions of the C5–6 FJC shown in Fig. 4B from Lu et al.,[28] cervical FJC maximum principal strain magnitudes were significantly correlated to joint distraction ($p<0.001$, $R^2 = 0.84$), a finding which supports the use of joint motion as a predictor of strain magnitude in the current study. Correlations between relative vertebral translations in goat cervical FJCs and strain magnitude were higher compared to correlations between IVA and strain magnitude in the current study. Relative translations were not examined in the current study because there were no data in the prior human study for comparison.

Data from the current study support the concept that the FJC can function proprioceptively during physiological motions of the lumbar spine. The regression relationships developed in the current study were used to estimate cat and human IVA magnitudes that would correspond to 5% and 10% strain. These strain magnitudes represent those likely to be above the threshold needed to stimulate low-threshold, Group II mechanoreceptors.[13–14] The estimated IVA magnitudes that produced these strain magnitudes were within the range of motion for both cat and human spines during motions unrestricted by the articulating facets and that tensioned the FJC ligament (i.e., extension in the bilateral FJCs or right lateral bending in the right sided FJCs, see Table 3).

The potential proprioceptive role for the FJC highlights the importance of understanding how spinal motion affects the FJC at all spinal levels. Segmental hypomobility for example, a hallmark sign of spinal levels treated by chiropractors and osteopaths [29–30] presumably affects the FJC at distant segments as well. As seen in this study and numerous others,[31] regional lumbar motion is enabled by smaller motions of the individual lumbar vertebra. Should an individual segment become hypomobile, motion of the remaining segments must increase to accomplish the same regional motion. In experimental models where hypomobility is created using metal plates affixed to vertebral bodies, the greatest increase occurs in segments immediately above and below the hypomobile joint.[16, 32] Further, it has been shown that the resulting altered kinematics caused by segmental hypomobility resulted in altered patterns of FJC strains at the affected and adjacent joint levels.[16] We speculate that an altered strain pattern in turn adversely affects patterns of proprioceptive signaling wherein neural input from the FJC becomes incongruent with the regional motion.

During motions that are restricted by the articulating facets and that primarily compressed the FJC (i.e., extension in the bilateral FJCs or right lateral bending in the right sided FJCs), threshold strains (likely arising from shear) would be achieved at IVA magnitudes that were outside the range of motion for both cat and human spines. These data support the hypothesis that the FJC could function proprioceptively during spinal motions that induce tension on the FJC. Other ligamentous spinal structures such as the ligamentum flavum (which encloses the medial portion of the facet joint) are loaded in tension during ipsilateral lateral bending and extension, and it has been suggested that Group II and III proprioceptive afferents innervate the ligamentum flavum.[5]

Limitations

There are a number of constraints that should be considered when interpreting the results of the current study. First, data were collected using cadaveric spine specimens in the absence of surrounding tissue which might affect the relationship between FJC strain and kinematic measures. Either *in vitro* or *in vivo*, the passive properties of surrounding musculature could restrict spinal motions and result in smaller strain magnitudes. On the other hand, in the unanesthetized cat or human, contraction of multifidi muscles (which insert on capsule

surfaces) could result in larger FJC strains. Second, extrapolation of FJC afferent response from cat to humans is reliant upon the assumption that cat and human FJC neurons have similar strain thresholds. Measurement of responses from FJC neurons in humans is currently not feasible. However, appropriately designed testing, for example by specifically anesthetizing the facet joint capsule,[33] may help identify the specific role of human FJC afferents in spine proprioception. Third, similar to the prior study in human spines, the experimental model used in the current study was run under displacement control and without axial compression which could affect the relationship between IVA and capsule strain. Despite the fact that cats are quadrupedal and humans bipedal, biomechanical analyses of quadrupeds (i.e., free body diagrams and trabecular alignment) demonstrate that, like bipeds, their spines are also loaded axially in the neutral posture.[34] The lumbar lordosis in human spines is not present in cats, which could also result in different biomechanics between species. While the regression relationships established in the current study likely accounted for this, the influence of the lordosis in the human spine on FJC strain magnitude is unknown. Cat spines were matched for sex, age, and weight while human spines in the prior study represented an aged population from an uncontrolled set of donors. This may account for the increased variability in human strain data compared to cats. The regression relationship for humans also may not hold for younger spines, as observations in our laboratory (unpublished) indicate that human lumbar spines from younger donors are more flexible than those from an older population. Any of these factors could influence the generalized applicability of the regression relationships developed in the current study.

Conclusion

In conclusion, regression relationships between FJC strain and intervertebral angle during spinal motions were established for the lumbar spine in cat and human. Utility of the relationships was shown by estimating intervertebral angles in the cat and human that corresponded to FJC strains above the magnitude needed to activate low-threshold, Group II mechanoreceptor. These IVAs were within the range of motion for intersegmental motions that would be restricted by strain of the FJC. These data provide support for the role of the FJC and low threshold mechanoreceptive afferents in lumbar spine proprioception. Data obtained from the current study may be used to interpret future neuromechanical studies conducted in cat specimens that are designed to elucidate the FJC's role in lumbar spine proprioception, disease states (e.g., segmental hypomobility), and spinal manipulative therapy.

Acknowledgments

FUNDING SOURCES

This study was supported by funds from the National Institute of Health National Center for Complementary and Alternative Medicine (U19AT001701) and Ruth L. Kirschstein National Research Service Award (F31AT002666).

References

1. Ianuzzi A, Little JS, Chiu JB, Baitner A, Kawchuk G, Khalsa PS. Human lumbar facet joint capsule strains: I. During physiological motions. Spine J. Mar-Apr; 2004 4(2):141–152. [PubMed: 15016391]
2. Panjabi MM, Goel VK, Takata K. Physiologic strains in the lumbar spinal ligaments. An in vitro biomechanical study 1981 Volvo Award in Biomechanics. Spine (Phila Pa 1976). May-Jun; 1982 7(3):192–203. [PubMed: 6214027]
3. Cavanaugh JM, Ozaktay AC, Yamashita HT, King AI. Lumbar facet pain: biomechanics, neuroanatomy and neurophysiology. J Biomech. 1996; 29(9):1117–1129. [PubMed: 8872268]

4. McLain RF, Pickar JG. Mechanoreceptor endings in human thoracic and lumbar facet joints. Spine. 1998; 23(2):168–173. [PubMed: 9474721]
5. Yamashita T, Cavanaugh JM, el Bohy AA, Getchell TV, King AI. Mechanosensitive afferent units in the lumbar facet joint. J Bone Joint Surg Am. 1990; 72(6):865–870. [PubMed: 2365719]
6. Cavanaugh JM, Ozaktay AC, Yamashita T, Avramov A, Getchell TV, King AI. Mechanisms of low back pain: a neurophysiologic and neuroanatomic study. Clin Orthop. 1997; (335):166–180. [PubMed: 9020216]
7. Pickar JG. Neurophysiological effects of spinal manipulation. Spine J. Sep-Oct; 2002 2(5):357–371. [PubMed: 14589467]
8. Pickar JG. An in vivo preparation for investigating neural responses to controlled loading of a lumbar vertebra in the anesthetized cat. J Neurosci Methods. 1999; 89(2):87–96. [PubMed: 10491938]
9. Pickar JG, McLain RF. Responses of mechanosensitive afferents to manipulation of the lumbar facet in the cat. Spine. 1995; 20(22):2379–2385. [PubMed: 8578387]
10. Pickar JG, Kang YM. Paraspinal muscle spindle responses to the duration of a spinal manipulation under force control. J Manipulative Physiol Ther. Jan; 2006 29(1):22–31. [PubMed: 16396726]
11. Ianuzzi A, Khalsa PS. Comparison of human lumbar facet joint capsule strains during simulated high-velocity, low-amplitude spinal manipulation versus physiological motions. Spine J. May-Jun; 2005 5(3):277–290. [PubMed: 15863084]
12. Ianuzzi A, Pickar JG, Khalsa PS. Validation of the cat as a model for the human lumbar spine during simulated high-velocity, low-amplitude spinal manipulation. J Biomech Eng. Jul.2010 132(7):071008. [PubMed: 20590286]
13. Khalsa PS, Hoffman AH, Grigg P. Mechanical states encoded by stretch-sensitive neurons in feline joint capsule. J Neurophysiol. 1996; 76(1):175–187. [PubMed: 8836217]
14. Little JS, Khalsa PS. Material properties of the human lumbar facet joint capsule. J Biomech Eng. 2005; 127(1):15–24. [PubMed: 15868784]
15. Ianuzzi A, Pickar JG, Khalsa PS. Determination of torque-limits for human and cat lumbar spine specimens during displacement-controlled physiological motions. Spine J. Jan-Feb; 2009 9(1):77–86. [PubMed: 17983845]
16. Little JS, Ianuzzi A, Chiu JB, Baitner A, Khalsa PS. Human lumbar facet joint capsule strains: II. Alteration of strains subsequent to anterior interbody fixation. Spine J. Mar-Apr; 2004 4(2):153–162. [PubMed: 15016392]
17. Little JS, Khalsa PS. Human lumbar spine creep during cyclic and static flexion: creep rate, biomechanics, and facet joint capsule strain. Ann Biomed Eng. 2005; 33(3):391–401. [PubMed: 15868730]
18. Ianuzzi A, Zambrano I, Tataria J, Ameerally A, Agulnick M, Goodwin JS, et al. Biomechanical evaluation of surgical constructs for stabilization of cervical teardrop fractures. Spine J. Sep-Oct; 2006 6(5):514–523. [PubMed: 16934720]
19. Dekutoski MB, Schendel MJ, Ogilvie JW, Olsewski JM, Wallace LJ, Lewis JL. Comparison of in vivo and in vitro adjacent segment motion after lumbar fusion. Spine (Phila Pa 1976). Aug 1; 1994 19(15):1745–1751. [PubMed: 7973970]
20. Soderkvist I, Wedin PA. Determining the movements of the skeleton using well-configured markers. J Biomech. 1993; 26(12):1473–1477. [PubMed: 8308052]
21. Gaudette GR, Todaro J, Krukenkamp IB, Chiang FP. Computer aided speckle interferometry: a technique for measuring deformation of the surface of the heart. Ann Biomed Eng. 2001; 29(9): 775–780. [PubMed: 11599585]
22. Hatze H. High-precision three-dimensional photogrammetric calibration and object space reconstruction using a modified DLT-approach. J Biomech. 1988; 21(7):533–538. [PubMed: 3410856]
23. Winkelstein BA, Nightingale RW, Richardson WJ, Myers BS. The cervical facet capsule and its role in whiplash injury: a biomechanical investigation. Spine. 2000; 25(10):1238–1246. [PubMed: 10806500]

24. Ianuzzi A, Khalsa PS. High loading rate during spinal manipulation produces unique facet joint capsule strain patterns compared with axial rotations. J Manipulative Physiol Ther. Nov-Dec; 2005 28(9):673–687. [PubMed: 16326237]
25. Glantz, SA.; Slinker, BK. Primer of applied regression and analysis of variance. Vol. 2. New York: McGraw-Hill, Inc; 2004. Mixing continuous and categorical variables: Analysis of covariance; p. 241-273.
26. Macpherson JM, Ye Y. The cat vertebral column: stance configuration and range of motion. Exp Brain Res. 1998; 119(3):324–332. [PubMed: 9551833]
27. Panjabi MM, Oxland TR, Yamamoto I, Crisco JJ. Mechanical behavior of the human lumbar and lumbosacral spine as shown by three-dimensional load-displacement curves. J Bone Joint Surg Am. 1994; 76(3):413–424. [PubMed: 8126047]
28. Lu Y, Chen C, Kallakuri S, Patwardhan A, Cavanaugh JM. Neurophysiological and biomechanical characterization of goat cervical facet joint capsules. J Orthop Res. 2005; 23(4):779–787. [PubMed: 16022990]
29. Kuchera, WA.; Kappler, RE. Musculoskeletal examination for somatic dysfunction. In: Ward, RC.; Hruby, RJ.; Jerome, JA.; Jones, JM.; Kappler, RE., editors. Foundations for Osteopathic Medicine. Lippincott: Williams & Wilkins; 2002. p. 633-659.
30. Sportelli, L.; Tarola, G. Documentation and record keeping. In: Halderman, S.; Dagenais, S.; Budgell, B., et al., editors. Principles and Practice of Chiropractic. New York: McGraw-Hill; 2005. p. 725-741.
31. White, AA.; Panjabi, MM. Clinical Biomechanics of the Spine. Philadelphia: JB Lippincott; 1990.
32. Ragab AA, Escarcega AJ, Zdeblick TA. A quantitative analysis of strain at adjacent segments after segmental immobilization of the cervical spine. J Spinal Disord Tech. Aug; 2006 19(6):407–410. [PubMed: 16891975]
33. Kaplan M, Dreyfuss P, Halbrook B, Bogduk N. The ability of lumbar medial branch blocks to anesthetize the zygapophysial joint. A physiologic challenge. Spine (Phila Pa 1976). Sep 1; 1998 23(17):1847–1852. [PubMed: 9762741]
34. Smit TH. The use of a quadruped as an in vivo model for the study of the spine - biomechanical considerations. Eur Spine J. 2002; 11(2):137–144. [PubMed: 11956920]

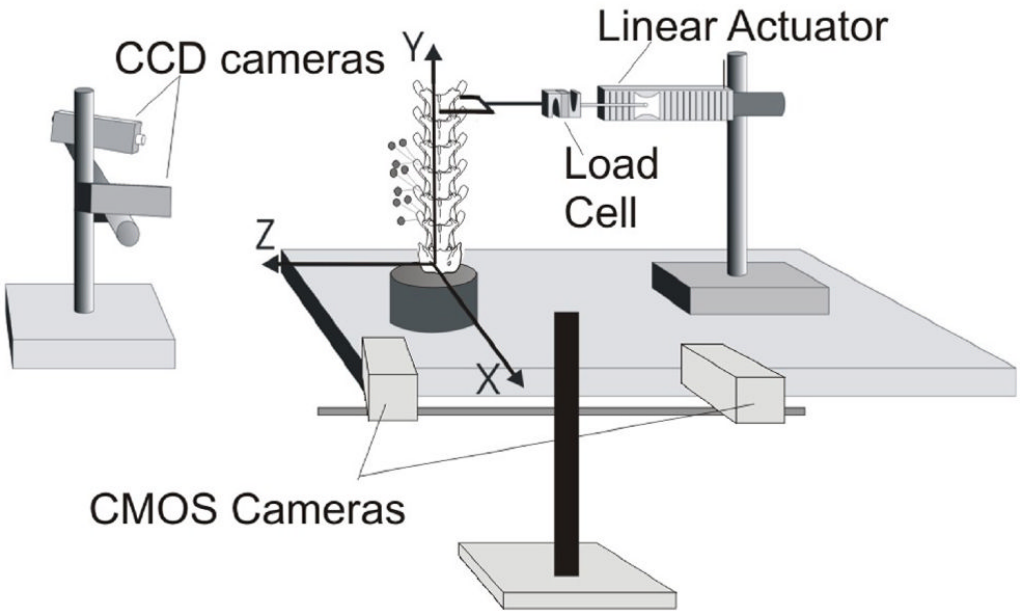

Figure 1.
Schematic of the experimental setup for measuring cat lumbar facet joint capsule strain magnitudes during extension, flexion and lateral bending. Coordinate axes are shown, with positive x-, y- and z-axes oriented in the posterior, cephalic and left directions, respectively. L5 through L7 vertebral kinematics were measured by optically tracking, with two CCD cameras, the 3D displacements of markers attached to the transverse processes. Facet joint capsule strain measurements were taken by imaging the capsule of interest using two CMOS cameras.

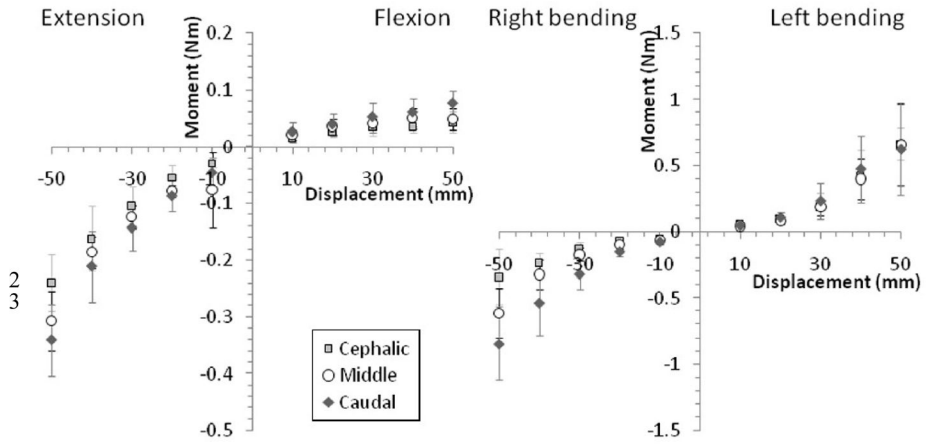

Figure 2.

Joint moment at the cat cephalic (L5–6), middle (L6–7) and caudal (L7-S1) joints versus global spine displacement during spinal motions of extension-flexion (left graph) and lateral bending (right graph). Error bars show standard deviations. Note difference in y-axis scaling.

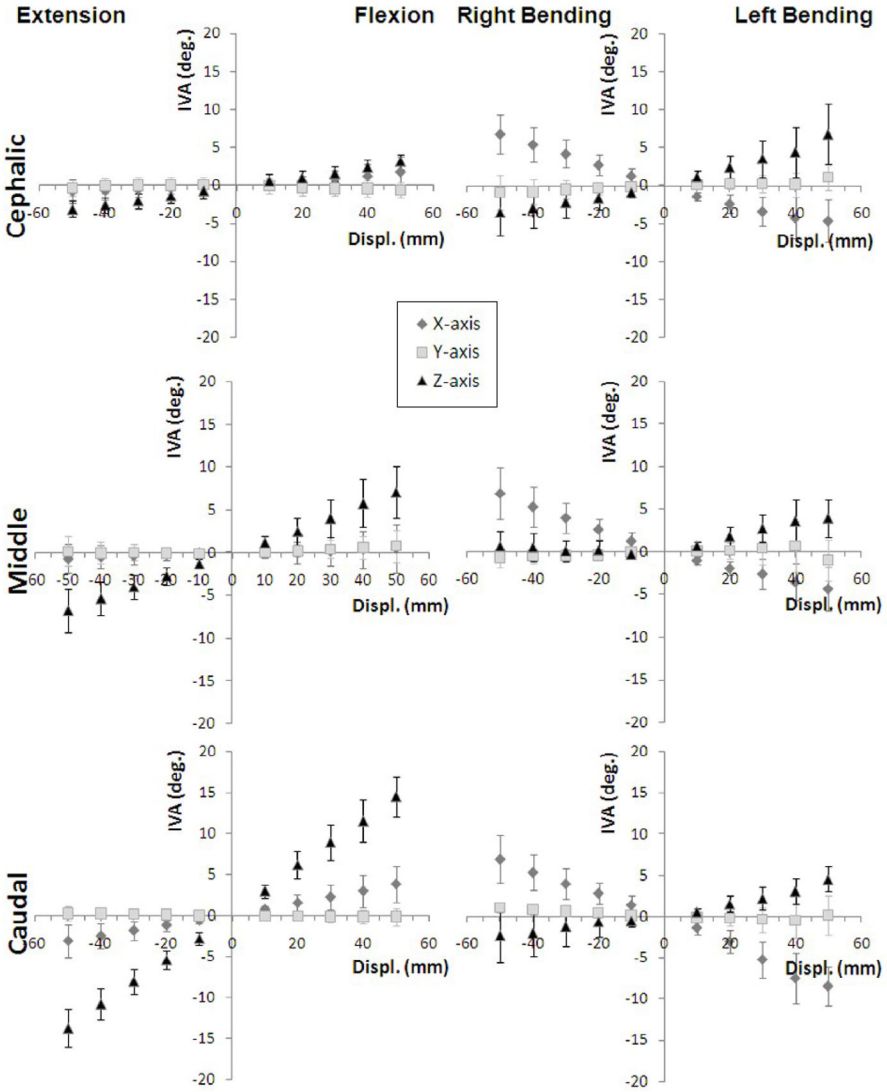

Figure 3.
Cat intervertebral angle (IVA) at the cephalic (L5–6), middle (L6–7) and caudal (L7-S1) joints during spinal motions of extension-flexion and lateral bending.

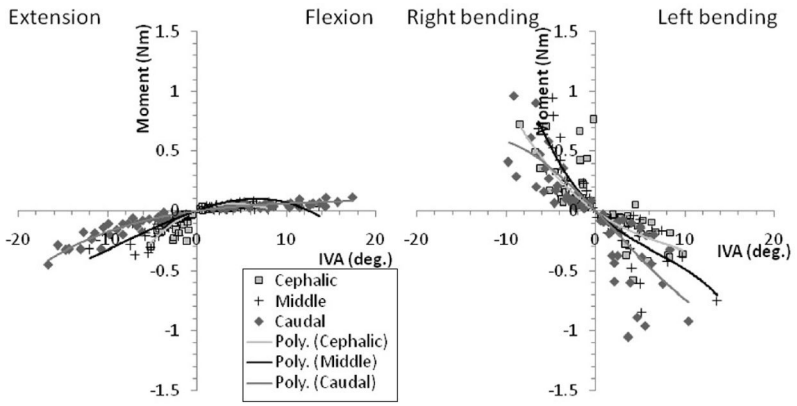

Figure 4.
Cat spine joint moment - intervertebral angle (IVA) polynomial (Poly.) relationships at the cephalic (L5–6), middle (L6–7) and caudal (L7-S1) joints during spinal motions of extension- flexion and lateral bending. Note the difference in axis scale.

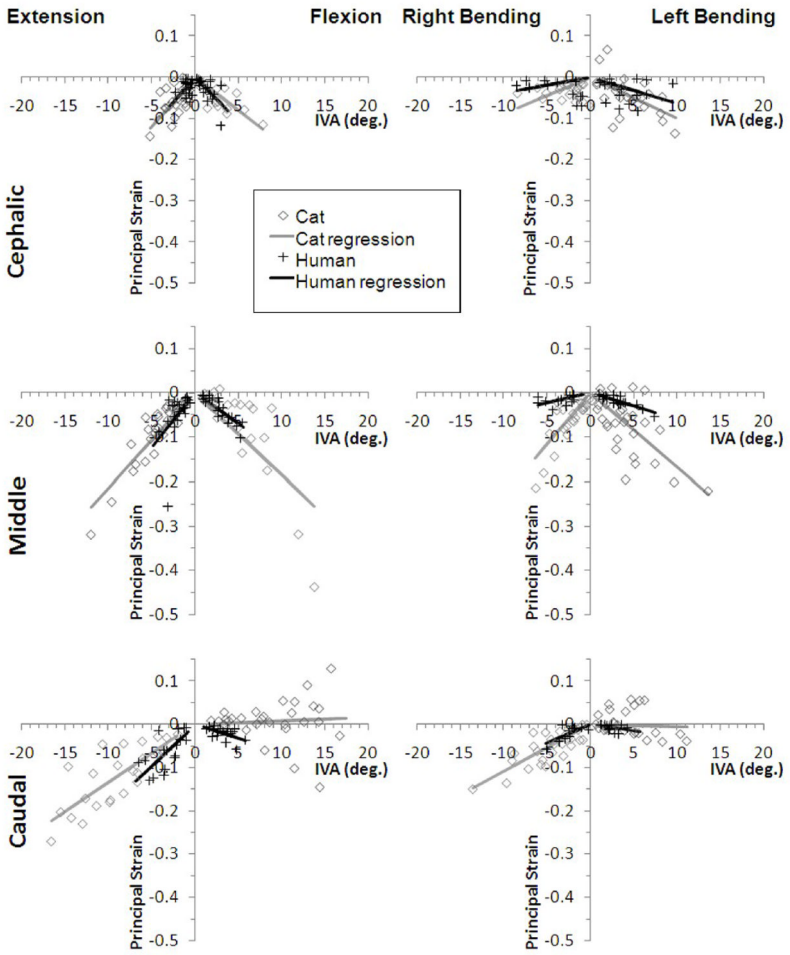

Figure 5.

Cat and human minimum principal strain magnitudes ($\hat{E}_2$) as a function of intervertebral angle (IVA) during extension-flexion and lateral bending. Linear regression relationships are shown for the cephalic (human L3–4, cat L5–6), middle (human L4–5, cat L6–7) and caudal (human L5-S1, cat L7-S1) joints.

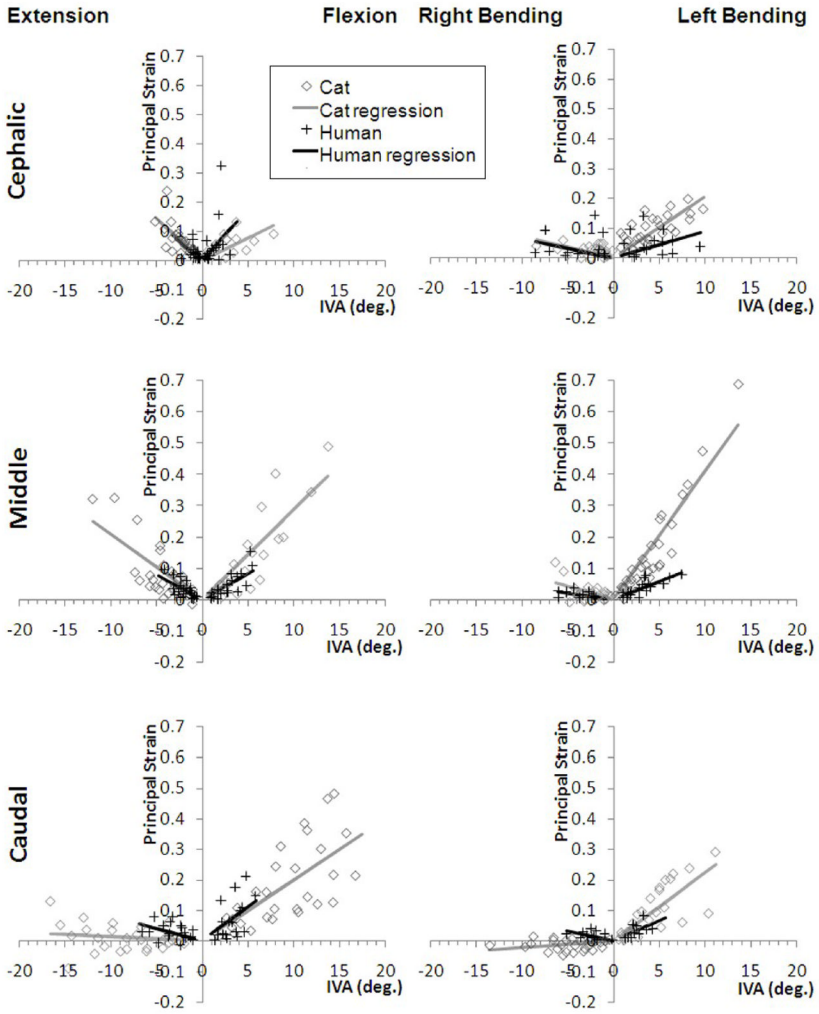

Figure 6.

Cat and human maximum principal strain magnitudes ($\hat{E}_1$) as a function of intervertebral angle (IVA) during extension-flexion and lateral bending. Linear regression relationships are shown for the cephalic (human L3–4, cat L5–6), middle (human L4–5, cat L6–7) and caudal (human L5-S1, cat L7-S1) joints.

Table 1

Linear regression coefficients (slope estimates) for $\hat{E}_2$ vs. IVA relationships.

Joint Level	Motion	Cat			Human			A_C/A_H
		Estimate (A_C)	p-value	R^2	Estimate (A_H)	p-value	R^2	
Cephalic	Extension	0.024	<0.001	0.35	0.024	<0.001	<0.01	1.00
Cephalic	Flexion	−0.016	<0.001	0.47	−0.021	<0.001	0.42	0.76
Cephalic	Left Bend	−0.010	<0.001	0.36	−0.006	0.003	<0.01	1.67
Cephalic	Right Bend	0.009	<0.001	<0.01	0.004	0.12	0.43	2.25
Middle	Extension	0.021	<0.001	0.86	0.025	<0.001	0.26	0.84
Middle	Flexion	−0.018	<0.001	0.70	−0.014	<0.001	0.81	1.29
Middle	Left Bend	−0.017	<0.001	0.42	−0.006	<0.001	0.79	2.83*
Middle	Right Bend	0.023	<0.001	0.55	0.004	<0.001	0.11	5.75*
Caudal	Extension	0.013	<0.001	0.62	0.019	<0.001	0.44	0.68*
Caudal	Flexion	0.001	0.41	<0.01	−0.006	<0.001	0.24	−0.17*
Caudal	Left Bend	−0.001	0.58	0.08	−0.003	0.01	0.12	0.33
Caudal	Right Bend	0.011	<0.001	0.63	0.009	<0.001	0.50	1.22

* Indicates significant difference in slopes, $p<0.05$

Table 2

Regression coefficients (slope estimates) for $\hat{E}_1$ vs. IVA relationships.

Joint Level	Motion	Cat			Human			A_C/A_H
		Estimate (A_C)	p-value	R2	Estimate (A_H)	p-value	R2	
Cephalic	Extension	−0.029	<0.001	0.52	−0.025	<0.001	0.05	1.16
Cephalic	Flexion	0.016	<0.001	0.16	0.035	0.005	0.07	0.46
Cephalic	Left Bend	0.021	<0.001	0.53	0.009	0.003	<0.01	2.33*
Cephalic	Right Bend	−0.007	<0.001	0.04	−0.006	0.07	<0.01	1.17
Middle	Extension	−0.021	<0.001	0.60	−0.016	<0.001	0.43	1.31
Middle	Flexion	0.029	<0.001	0.79	0.017	<0.001	0.66	1.71*
Middle	Left Bend	0.041	<0.001	0.90	0.012	<0.001	0.62	3.42*
Middle	Right Bend	−0.008	<0.001	0.27	−0.004	<0.001	0.21	2.00*
Caudal	Extension	−0.001	0.14	0.07	−0.008	<0.001	0.06	0.13*
Caudal	Flexion	0.020	<0.001	0.47	0.023	<0.001	0.29	0.87
Caudal	Left Bend	0.022	<0.001	0.58	0.013	<0.001	0.29	1.69*
Caudal	Right Bend	0.002	0.002	<0.01	−0.006	0.001	0.06	−0.33*

* Indicates significant difference in slopes, $p<0.05$

Table 3

Utilization of the linear regression relationships to estimate IVA magnitudes (in degrees) required to achieve 5% and 10% FJC strain. Entries shaded in grey indicate IVA estimates that exceeded the motion of the cat or human spines.

Joint Level	Motion	Cat					Human				
		Range of Motion (deg)	Estimated IVA		Estimated IVA		Range of Motion (deg)	Estimated IVA		Estimated IVA	
			Tensile Strain		Compressive Strain			Tensile Strain		Compressive Strain	
			5%	10%	5%	10%		5%	10%	5%	10%
Cephalic	Extension	−3.3±1.6	−1.7	−3.4	−2.1	−4.2	−1.7±0.9	−2.0	−4.0	−2.1	−4.2
Cephalic	Flexion	5.0±2.0	3.1	6.3	3.1	6.3	2.7±0.9	1.4	2.9	2.4	4.8
Cephalic	Left Bend	6.8±2.3	2.4	4.8	5.0	10.0	6.9±1.8	5.6	11.1	8.3	16.7
Cephalic	Right Bend	−4.0±2.9	−7.1	−14.3	−5.6	−11.1	−6.3±2.5	−8.3	−16.7	−12.5	−25.0
Middle	Extension	−6.9±2.7	−2.4	−4.8	−2.4	−4.8	−3.1±0.7	−3.1	−6.3	−2.0	−4.0
Middle	Flexion	7.6±3.8	1.7	3.4	2.8	5.6	4.6±1.0	2.9	5.9	3.6	7.1
Middle	Left Bend	6.9±3.7	1.2	2.4	2.9	5.9	5.1±1.7	4.2	8.3	8.3	16.7
Middle	Right Bend	−4.3±2.6	−6.3	−12.5	−2.2	−4.3	−4.7±1.7	−12.5	−25.0	−12.5	−25.0
Caudal	Extension	−14.4±2.1	−50.0	−100.0	−3.8	−7.7	−5.3±1.3	−6.3	−12.5	−2.6	−5.3
Caudal	Flexion	14.8±2.5	2.5	5.0	−50.0	−100.0	4.8±0.8	2.2	4.3	8.3	16.7
Caudal	Left Bend	7.4±3.2	2.3	4.5	50.0	100.0	3.9±1.6	3.8	7.7	16.7	33.3
Caudal	Right Bend	−7.5±1.7	25.0	50.0	−4.5	−9.1	−3.1±1.4	−8.3	−16.7	−5.6	−11.1

IVA, intervertebral angle; FJC, facet joint capsule